Application of Damage Detection of Steel Structure Lamb Wave Modal Superposition Imaging Based on Scanning Laser Vibration Measurement

ZIPING WANG[1*], BINGQIAN LI[1], HANGRUI CUI[1],
ANTONIO FERNÁNDEZ-LÓPEZ[2] and ALFREDO GÜEMES[2,*]

ABSTRACT:

Due to their high strength, high-temperature resistance, good toughness, and plasticity, steel structural plates are widely used in major engineering structures such as high-speed rail, vehicles, and civil engineering. However, they are easily damaged by external loads and impacts during long-term service. Aiming at the shortcomings of dispersion and multi-modal effects in the current Lamb wave detection, and since damage information cannot be effectively identified, this paper studies, through simulation and experiments, the Lamb wave driven by a sinusoidal modulation five-peak wave signal in a steel structure plate with flat-bottomed holes. The finite element numerical model of the propagation was established, and the corresponding damage detection experimental platform including steel and aluminum boards was built. The experimental data were obtained by Scanning Laser Doppler Vibrometer (SLDV). It can be seen from the experimental results that under the condition of the same frequency, the damage reflection energy of the two different modes is relatively obvious. Through the data fusion of the two modes, the results obtained are more accurate than the damage imaging results of the single mode in the frequency wavenumber (*f*-*k*) domain. Finally, the damage location experiment of one through hole in the steel board and the double flat bottom holes in aluminum plate are carried out to verify the feasibility of the algorithm in isotropic plate.

1. INTRODUCTION

As one of the first types of structures which was used in early engineering structures in the world, steel plate structures are widely used because of their high strength, light weight, fast construction speed, and good seismic performance [1,2]. With the rapid development of my country's urbanization and the rise of my country's steel production to the forefront of the world, the advantages of steel plate structures in terms of comprehensive economic benefits and earthquake resistance have been more and more widely recognized

[1]Faculty of Civil Engineering and Mechanics, Jiangsu University and National Center for International Research on Structural Health Management of Critical Components, Zhenjiang, China,

[2]Department of Aeronautics， Polytechnic University of Madrid, Madrid, Spain

* Correspondence: wzpxx2004@126.com, alfredo.guemes@upm.es

[3]. In the long-term service process, it's easy to produce fatigue, spalling, and other damage. The technology based on ultrasonic guided waves has shown great application potential in non-destructive testing [4-6].

Achenbach [7] and Graff [8] first studied the dispersion equation of Lamb waves in isotropic plates and plotted the dispersion curve. In 1991, Alleyne D [9] proposed an analysis method for multi-mode transmission signals, showing the effectiveness of two-dimensional Fourier transform (2D FFT) method for identifying and measuring single modes. In 2003, Benz [10] used time-frequency imaging technology to analyze the interaction between multi-mode and dispersion of Lamb waves propagating in a grooved plate. Based on this, the groove defects were located. In 2007, Ruzzene [11] successfully separated the direct signal and scattered signal of single mode of Lamb wave by using filtering technology in *f-k* domain.

In 2009, Wang [12] proposed a wave packet reconstruction method for the problem of Lamb wave damage imaging. The experiments showed that the method can effectively eliminate the wave packet aliasing phenomenon in the monitoring signal. The accuracy of the active Lamb wave damage imaging method was improved. In 2014, Tian [13] gave a general description of the use of 2D and three-dimensional (3D) FFT to analyze wave motion theorem and modal filtering. Frequency and mode filtering are realized by a filtering window function in space. The decomposition of the modal Lamb wave was performed, and the validity of the modal decomposition was verified by the time-delay power spectrum.

In 2016, Golato [14] proposed a multimodal sparse reconstruction method for defect localization in thin plates by exploiting the sparsity of defects and the multimodality of Lamb wave propagation in plates. In 2019, Yang [15] used laser Doppler vibrometer to collect time-space domain signals, and converted them into f-k domain through 3D FFT. A window function similar to an arc is designed to obtain the damage scattering wave of a single Lamb wave mode, and the phased array method is used to locate the damage.

In 2020, Zhang [16] used linear phased array imaging method in *f-k* domain to achieve S0 mode double damage imaging. Compared with time domain full focus method (TFM), it has higher resolution. In the same year, R. Gorgin [17] proposed a procedure for damage identification and characterization based on the principal curvature of the first mode of the plate. A change in the mode shape of the structure due to a change in geometry due to cracks or material degradation was exploited for damage identification. In 2022, Wang [18] proposed a mode decomposition imaging (MDI) algorithm for detecting delamination defects in carbon fiber composite panels using air-coupled Lamb waves, which includes the mode decomposition process and rotational scanning defect probability imaging. The method is more suitable for analyzing nonlinear non-stationary leaky Lamb wave signals. Recently, our research group [19-20] studied damage imaging using the common source method (CSM) time domain and *f-k* domain imaging for phased arrays.

In summary, guided waves have obvious advantages in the monitoring of

damage in plate structures. However, for different modes, the existing research has ignored their sensitivity to damage identification, and most of the damages are through-hole damage. There is less research on detection of the resulting flat bottom hole damage by impact. Therefore, on the basis of previous research, using multiple modes for damage imaging by studying the simulation and experiment of damage with prefabricated flat bottom holes was proposed. The experimental data were obtained by SLDV. The approach can consider the effects of different modes of guided wave very thoughtfully. The modalities imaging results are comprehensively weighted, thereby further improving the damage imaging accuracy and improving the shortcomings of the traditional single-modal damage imaging accuracy.

2. THE PRINCIPLE OF SUB-MODAL SUPERPOSITION IMAGING IN THE *F-K* DOMAIN

The modal separation in the *f-k* domain mainly includes two key links. One is to convert the signal from the time domain to the *f-k* domain by 3D FFT. Another is to construct a 3D window function in *f-k* domain to obtain a single-mode guided wave. Generally, at low frequencies, only S_0 and A_0 modes will appear in ultrasonic Lamb waves. Therefore, the above two modes were taken as the analysis content in the paper. The separation of the two modes is achieved by constructing appropriate 3D window functions in the f-k domain.

Figure 1 is a flow chart of the sub-modal stack imaging method in *f-k* domain. Firstly, the simulation model/experiment platform is built, and receive guided wave data with SLDV, which is transformed into an *f-k* domain matrix by 3D FFT. Then, it is windowed by the constructed 3D window function to achieve modal separation. The *f-k* domain imaging is performed on the separated single modality. Finally, the modal overlay imaging is realized by data fusion of the imaging images of different modalities [21].

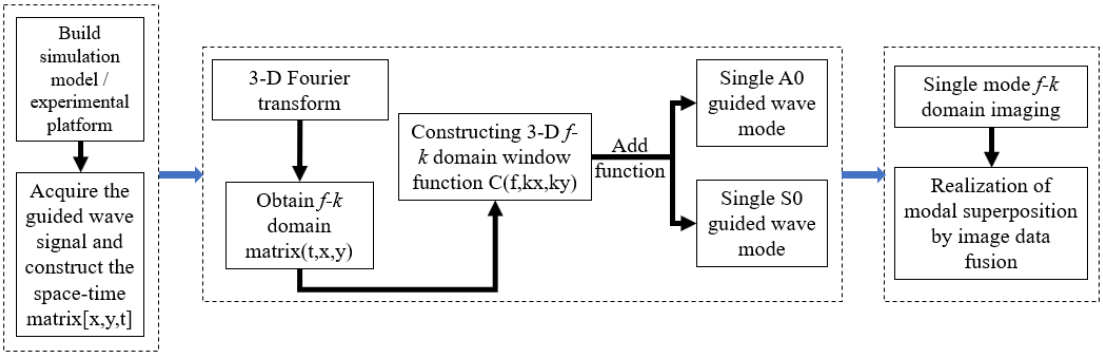

Figure 1 Flow chart of the method for sub-modal stacking imaging in the *f-k* domain

2.1 3D FFT

For the propagation of Lamb waves in thin plates, 3D FFT [22] can be used to analyze the wave field information. The 3D FFT of 2D guided wave propagation problem is shown in equation (1)

$$A(f,k_x,k_y)=\int_{-\infty}^{\infty}\int_{-\infty}^{\infty}\int_{-\infty}^{\infty}a(t,x,y)e^{-i(2\pi ft-k_xx-k_yy)}d(t)d(x)d(y) \tag{1}$$

where *kx* and *ky* are wave number vectors along the *x* and *y* directions respectively, *t* represents the variable in time and *f* represents the variable in frequency. Its inverse transformation is as follows

$$a(t,x,y)=\frac{1}{(2\pi)^2}\int_{-\infty}^{\infty}\int_{-\infty}^{\infty}\int_{-\infty}^{\infty}A(f,k_x,k_y)e^{i(2\pi ft-k_xx-k_yy)}d(f)d(k_x)d(k_y) \tag{2}$$

Convert the acquired time-domain signal *a*(*x, y, t*) to *f-k* domain signal *A*(*f, kx , ky*) through 3D FFT. According to the correspondence between the wavefield information and the *f-k* matrix [23], the extraction of guided wavefields in different directions can be realized by selecting the desired quadrants in the *f-k* matrix obtained after 3D FFT. Then the time domain waveform can be obtained through the 3D inverse FFT.

2.2 3D *f-k* Domain Window Function Design

To retain the desired frequency and wavenumber components, it is necessary to design a band-pass filter in the *f-k* space. As shown in Formula (3):

$$C(f,k_x,k_y)=c(f)c(f,k_x,k_y)$$

(3)

where, *c(f)* is a cosine window function, which can select different central frequencies in the frequency domain. *C*(*f, kx, ky*) is the *f-k* domain window function for sub-modal, as shown in the following formula

$$c(f,k_x,k_y)=\begin{cases}\frac{1}{2}[1+\cos(\pi\frac{K_k(f,k_x,k_y)}{K_f})] & if\ \ \mathrm{K}_k(f,k_x,k_y)\le K_f\\ 0 & else\end{cases}$$

(4)

where k_f is the designed window width, and K_k(*f, kx, ky*) is as follows

$$K_k(f,k_x,k_y)=|k|-k_{ref}(f)$$

(5)

where $|k|=\sqrt{k_x^2+k_y^2}$, and $k_{ref}(f)$ is a reference signal, which can use the average value of theoretical value, simulation or experimental results as a reference. So the signal processing is as follows

$$A_w(f,k_x,k_y) = A(f,k_x,k_y)C(f,k_x,k_y)$$

(6)

We can extract signals of various guided wave modes through equation (4) and analyze them to achieve damage imaging.

3. Numerical simulation

3.1 Model Parameter Settings

The damaged steel plate model is shown in Figure 2, with a geometric dimension of 200 ×200 ×1 mm. The flat bottom hole damage is located in the upper right corner, the size is 6 mm, the depth is 0.7 mm, and its coordinates are (60 mm, 40 mm). The red part is the area where the guided wave signal data is scanned and received, and the rectangular array is used.The size of the collection area is 40 × 40 mm, and the distance between the array elements is 1 mm. The excitation signal is a five-peak waveform signal with a center frequency of 250 kHz. The boundary of the simulation model is set with a low reflection boundary and a Rayleigh damping absorption layer with a width of 5 mm to achieve the purpose of weakening the boundary reflection.

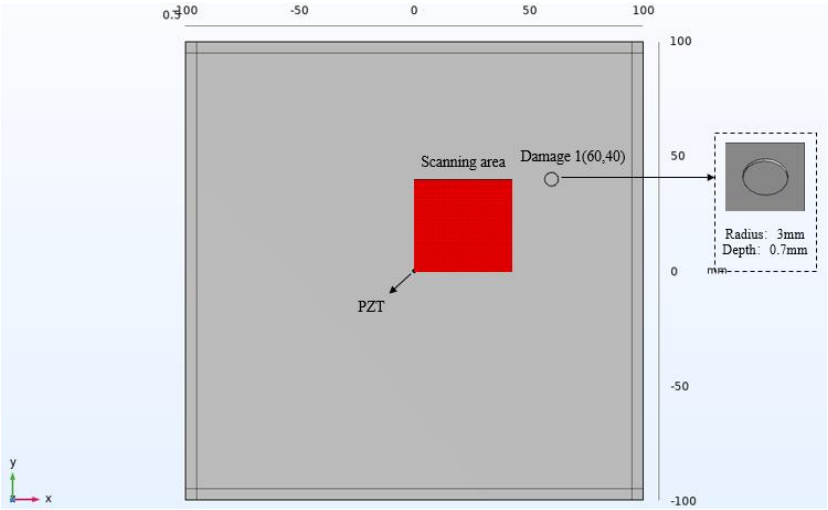

Figure 2. COMSOL model of a steel plate with flat-bottomed holes

3.2 Simulation Results and Analysis of *f-k* Domain Sub-Modal Superposition Imaging

The modal separation of the signal is carried out by the constructed 3D window

function, and extract single mode reflection signal. In Figure 3(a) to (c), they are time domain signals of an array unit and single A_0 and S_0 mode respectively, and are normalized. It can be seen that different modes are effectively separated. Figure 3(d) is the time-domain waveform of the removed direct wave. Figure 3 (e) and (f) are the reflection waves of A_0 and S_0 modes respectively. The first wave packet is damage scattering, and the others are boundary scattering.

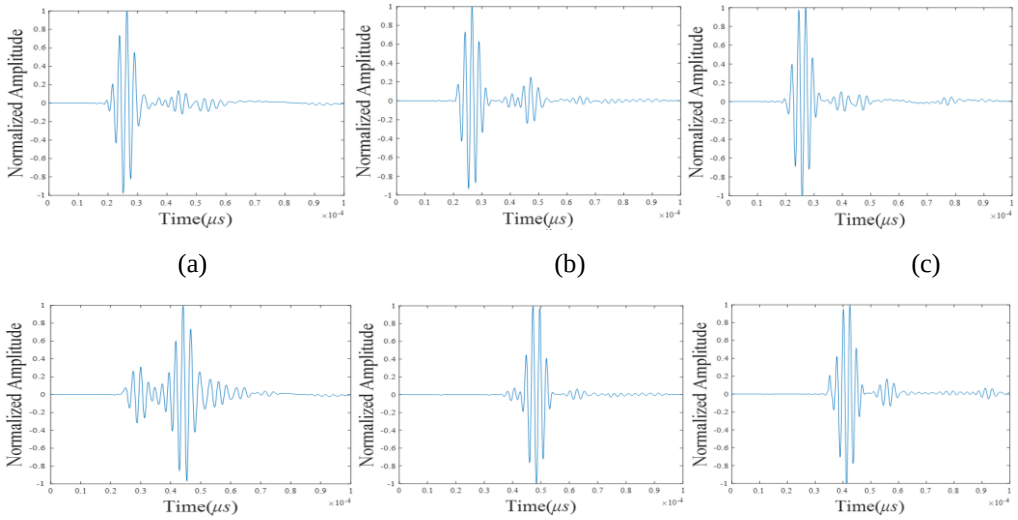

(a) (b) (c)

(d) (e) (f)

Figure 3 Waveform diagram of array element in time domain: (a) original waveform of an array element, (b) single A_0 modal, (c) single S_0 modal, (d) reflected waveform of an array element, (e) A_0 modal reflected waveform, (f) S_0 modal reflection waveform

The imaging results in the *f-k* domain are shown in Figure 4, the position of the black circle is the real damage position. Figure 4 (a) and (b) show the *f-k* imaging results of single A_0 and S_0 modes respectively. Figures 4(c) to (e) show the imaging results in the *f-k* domain by the amplitude stacking method, the amplitude stacking multiplication method, and the combined method of the amplitude adding and multiplying. It can be seen from the figure that the damage localization of the combined method of amplitude stacking and multiplication is more effective that of the amplitude stacking method, and its damage imaging area is smaller and more accurate.

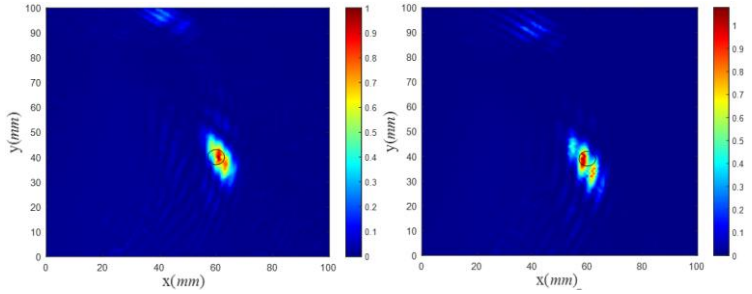

(a) (b)

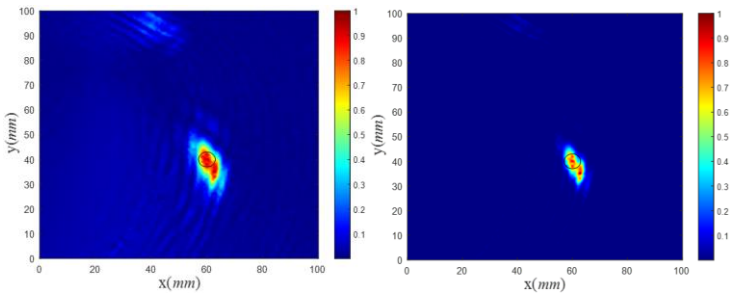

(c) (d)

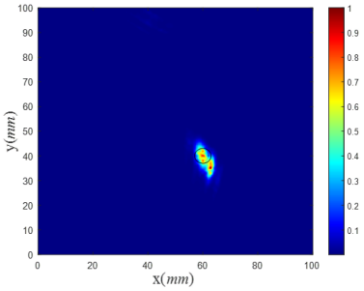

(e)

Figure 4 Imaging results in *f-k* domain: (a) single A_0 modal; (b) single S_0 modal; (c) S_0, A_0 modal amplitude stacking imaging results; (d) S_0, A_0 modal amplitude stacking imaging results; (e) the combined imaging result of S_0 and A_0 modal amplitudes.

By comparing the coordinates of the highest amplitude point in the image with the actual damage location, it can be seen that the coordinates with the highest amplitude point in a single A_0 modal image are (62, 40), and the resulting error is 2 mm. The coordinates of the highest point of the single S_0 modal imaging image amplitude are (58, 41), and the resulting error is 2.23 mm. After numerical fusion processing, the coordinates of the highest point of the damage imaging with the amplitude stacking damage imaging are (61, 41), and the resulting error is 1.41 mm. The coordinates of the highest amplitude of damage imaging obtained by the other two methods are (60,40), the error is negligible, and the damage location is accurate.

4. *F-k* domain sub-modal superposition imaging experiment

4.1 Experimental Setup

The excitation position of the steel plate, the size of the damage, and the position parameters in the experiment are shown in Table 1. The size of the steel plate selected in the experiment is 800×800mm. Let PZT position be the coordinate origin (0,0), the damage diameter is 10mm, and the central coordinate position is (120,120). First, the excitation signal is output through the signal generator and then output by the PZT after passing through the power

amplifier; secondly, the vibration signal of the corresponding scanning area on the steel plate is collected by the SLDV. The size of the signal collection area is 70×70mm. The element spacing is 1.4 mm.

TABLE.1 PARAMETER TABLE OF PZT AND DAMAGE LOCATION IN PLATE

Test subject	Size (mm^2)	PZT location (mm)	Damage center location (mm)	Damage diameter (mm)
Q235 steel plate	800×800	(0,0)	(120,120)	10

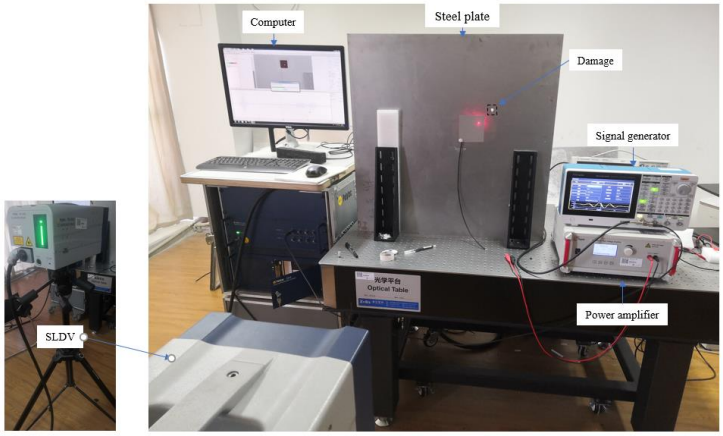

Figure 5 Schematic diagram of the isotropic steel plate sub-modal superposition imaging experimental platform

4.2 Experimental Results and Analysis of *f-k* Domain Sub-Modal Stack Imaging

The modal separation of the signal is carried out by the constructed 3D window function, and extract single mode reflection signal. In Figure 6(a) to (c), they are time domain signals of an array unit and single A_0 and S_0 mode respectively, and are normalized. It can be seen that different modes are effectively separated. Figure 6(d) is the time domain waveform of the removed direct wave. Figure 6 (e) and (f) are the reflection waves of A_0 and S_0 modes respectively. The first wave packet is damage scattering, and the others are boundary scattering.

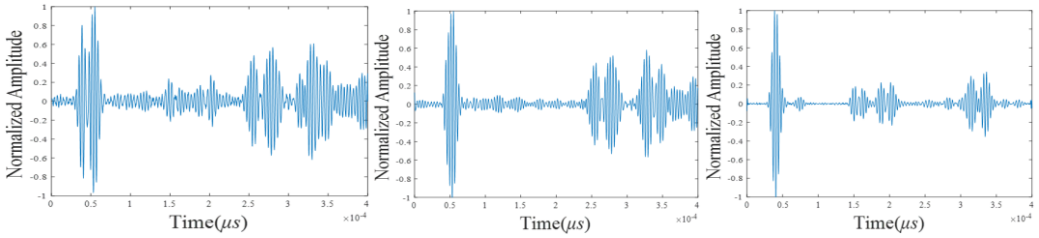

(a) (b) (c)

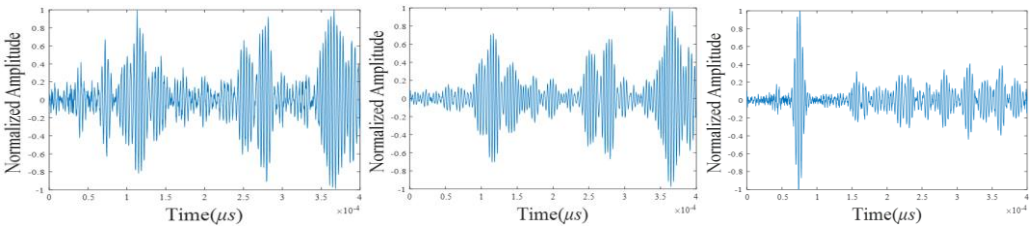

(d) (e) (f)

Figure 6 Waveform diagrams of array element in time domain: (a) original waveform of an array element, (b) single A_0 modal, (c) single S_0 modal, (d) reflected waveform of an array element, (e) A_0 modal reflected waveform, and (f) S_0 modal reflection waveform

The imaging results in the *f-k* domain are shown in Figure 7. Figure 7 (a) and (b) show the *f-k* imaging results of single A_0 and S_0 modes respectively. The damage range of S_0 mode imaging is larger than that of A_0 mode imaging range, and there are two darker positions with higher amplitudes and farther away from the actual damage. The overall error is large. The imaging results of different modalities are processed by numerical fusion. Figures 7(c) to (e) are the imaging results of the amplitude stacking method, the amplitude stacking multiplication method, and the combined method of the amplitude adding and multiplying in the *f-k* domain. Compared with the other two methods, the combined method of the amplitude adding and multiplying has higher accuracy for damage imaging.

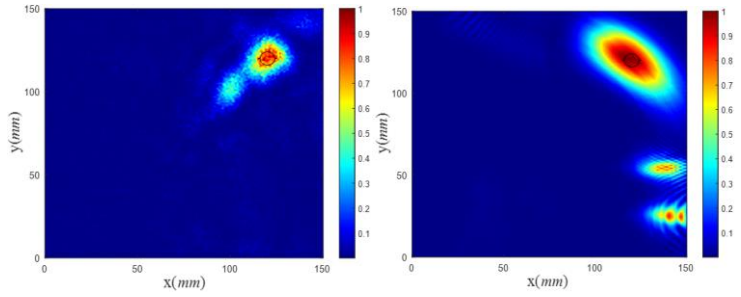

(a) (b)

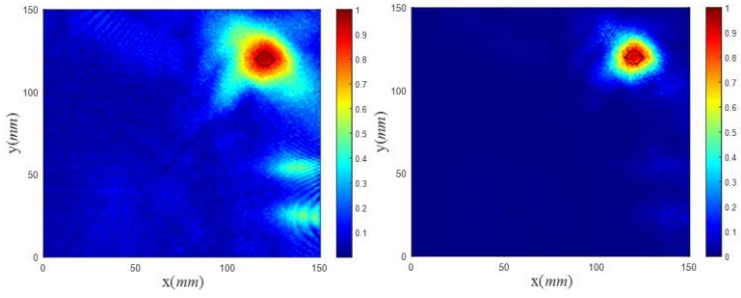

(c) (d)

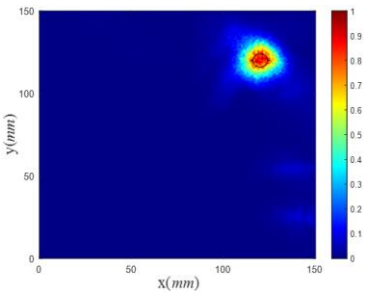

(e)

Figure 7 Imaging results in *f-k* domain: (a) single A_0 modal, (b) single S_0 modal, (c) S_0, A_0 modal amplitude stacking imaging results, (d) S_0, A_0 modal amplitude stacking imaging results, and (e) the combined imaging result of S_0 and A_0 modal amplitudes

By comparing the coordinates of the highest amplitude point in the imaging image with the actual damage location, it can be observed that the coordinates of the highest amplitude point in a single A_0 modal imaging image are (122,121), and the resulting error is 2.23 mm. The coordinates of the highest point of the single S_0 modal imaging image amplitude are (121, 121), and the result error is 1.41 mm. After numerical fusion processing, the coordinates of the highest point of the damage imaging with the amplitude stacking damage imaging are (121, 121), and the result error is 1.41 mm. The coordinates of the highest point of the damage imaging with the other two methods damage imaging are (120, 120), the error is negligible and the damage location is accurate. Obviously, the combined method of the amplitude adding and multiplying has the best imaging effect.

4.3 Experimental Results and Analysis of Aluminum Plate with Double Flat Bottom Holes

The size of the aluminum plate selected is 700mm×700mm×1mm,.Assume that the center position of the board is the origin of coordinates (0mm, 0mm), and paste PZT.The central coordinate positions of two flat bottom holes damage were (90mm, 90mm), (100mm, 50mm), the diameter of damage was 4mm, and the depth was 0.7mm(±0.03mm). The layout of the experimental platform is consistent with Section 4.1.

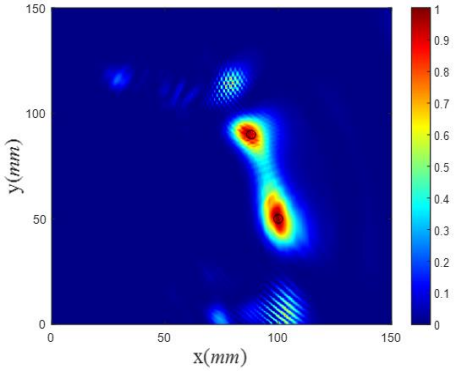

Figure 8 the combined imaging result of S_0 and A_0 modal amplitudes

The combined imaging result of S_0 and A_0 modal amplitudes in the *f-k* domain is shown in Figure 8.By comparing the coordinates of the highest amplitude of the damage area in the image with the actual damage location, it can be found that they are all located in the black circle, that is, within the actual damage range, and the damage location is accurate.

5. CONCLUSION

By constructing the finite element numerical model and building the corresponding damage detection experimental platform, and using SLDV to obtain the experimental data, the sub-modal damage imaging processing was carried out on the signals obtained from the simulation and experiment. The *f-k* domain modality imaging results are accurate for the identification of damage from flat bottom holes in steel structural plates and aluminum plates. After numerical fusion processing, the results show that the determined damage center is in good agreement with the actual damage center. Compared with single mode, the data fusion of the two modalities can improve the imaging accuracy of the damage, which verifies the feasibility and practicability of the algorithm. It is helpful to solve the problem of modal separation of multi-modal Lamb waves in sheet metal structures and the difficulty of identifying multiple small damages on the surface of the structure.

Declaration of Interest Statement

The authors declare no conflict of interest regarding the publication of this paper.

Acknowledgments

This work was supported by China Scholarship Council (No.202008320084), the National Natural Science Foundation of China (No.11872191 and No.12072133) and Technology Foreign Expert Project of Chinese Ministry of Science (DL2022014011L) and Postgraduate Research & Practice Innovation Programme of Jiangsu Province (KYCX22_3615).

Data Availability Statements

The data that support the findings of this study are available from the corresponding author upon reasonable request.

References

[1] Miki C. Use and Application of High-Performance Steels for Steel Structure. 2005.

[2] Wald F, Silva L, Moore D B, et al. Experimental behaviour of a steel structure under natural fire[J]. Fire Safety Journal, 2006, 41(7):509-522.

[3] Zhong T, He B. Developing new-type light-gage steel structure in China[J]. Engineering Science, 2000.

[4] Chang H Y, Yuan F G. Visualization of hidden damage from scattered wavefield reconstructed using an integrated high-speed camera system[J]. Structural Health Monitoring, 2020, (1):147592172094080.

[5] Sang S, Sandgren E, Wang Z. Wave attenuation and negative refraction of elastic waves in a single-phase elastic metamaterial[J]. Acta Mechanica, 2018.

[6] Chang H Y, Yuan F G. Damage imaging in a stiffened curved composite sandwich panel with wavenumber index via Riesz transform:[J]. Structural Health Monitoring, 2020, 19(3):902-916.

[7] Mendelsohn D A, Achenbach J D, and Keer L M, Scattering of Elastic-Waves by A Surface-Breaking Crack[J], Wave Motion, 1980, 3: 277-292.

[8] Rokhlin S I, Lewis D K, and Graff K F, Real-time study of frequency-dependence of attenuation and velocity of Ultrasonic-Waves during the curing reaction of epoxy-resin[J], Journal of the Acoustical Society of America, 1986, 6: 1786-1793.

[9] Alleyne, D. A two-dimensional Fourier transform method for the measurement of propagating multimode signals[J]. Journal of the Acoustical Society of America, 1991, 89(3):1159-1168.

[10] Benz, Rüdiger, Niethammer, et al. Localization of notches with Lamb waves.[J]. Journal of the Acoustical Society of America, 2003,114(2): 677-685.

[11] Ruzzene, M. Frequency-wavenumber domain filtering for improved damage visualization[J]. Smart Materials & Structures, 2007, 16(6): 2116.

[12] Wang Q, Yuan S F. Wave packet reconstruction method in active Lamb wave damage imaging monitoring [J]. Chinese Journal of Astronautics, 2009, 30(03): 1207-1211.

[13] Tian Z, Yu L. Lamb wave frequency-wavenumber analysis and decomposition[J]. Journal of Intelligent Material Systems and Structures, 2014, 25(9): 1107-1123.

[14] Golato A, Santhanam S, Ahmad F, et al. Multimodal sparse reconstruction in guided wave imaging of defects in plates[J]. Journal of Electronic Imaging, 2016, 25(4): 043013.

[15] Yang G Y. Extraction and imaging research of Lamb wave single mode damage scattering wavefield [J]. Electronic Science and Technology, 2019, 32(7): 21-27.

[16] Zhang H Y, Duan W H. Defect detection of thin aluminum plate in frequency-wavenumber domain [J]. Acoustics Technology, 2020, 39(04): 434-438.

[17] Gorgin R, Wang Z. Structural Damage Identification Based on Principal Curvatures of Mode Shape. 2020.

[18] Wang B, Shi W, Zhao B, et al. A modal decomposition imaging algorithm for ultrasonic detection of delamination defects in carbon fiber composite plates using air-coupled Lamb waves[J]. Measurement, 2022, 195: 111165.

[19] Sang S, Sandgren E. Study of in-plane wave propagation in 2-dimensional anisotropic elastic metamaterials[J]. Journal of Vibration Engineering & Technologies, 2019, 7: 63-72.

[20] Wang Z, Fei Y, Li B, et al. Research on the *f-k* Domain Multimodal Damage Detection Imaging Fusion Method in Metal Plate[J]. Transactions of the Indian Institute of Metals, 2022, 75(11): 2777-2786.

[21] Fei Y , Wang Z P, Zhou A , et al. Research on Mode Superposition Damage Imaging Method for Isotropic Materials[C]// 2020 15th Symposium on Piezoelectricity, Acoustic Waves and Device Applications (SPAWDA). 2021.

[22] Wu T Y, Ume I C. Fundamental study of laser generation of narrowband Lamb waves using superimposed line sources technique[J]. NDT & E International, 2011, 44(3): 315-323.

[23] Yang L, Ume I C. Application of 3-D FFT in laser ultrasonic NDT technique[C]//International Conference on Barkhausen & Micro-magnetics. American Institute of Physics 2014: 380-388.